Research Article

iMedPub Journals
www.imedpub.com

Journal of Imaging and Interventional Radiology

2020
Vol.3 No.1:1

DOI: 10.21767/2471-8564.3.1.1

Magnetic Resonance Guided High Intensity Focused Ultrasound (MrgHIFU) for Treating Recurrent Gynaecological Tumours: Effect of Pre-Focal Tissue Characteristics on Target Heating

Sharon L Giles[1*], Ian Rivens[2], Georgios Imseeh[3], Matthew RD Brown[4,5], Alexandra Taylor[3], Gail R ter Haar[2] and Nandita M deSouza[1]

[1]The CRUK Cancer Imaging Centre, The Institute of Cancer Research and Royal Marsden Hospital, London, UK

[2]Therapeutic Ultrasound, The Institute of Cancer Research, London, UK

[3]Gynae-Oncology Department, The Royal Marsden Hospital, London

[4] Pain Medicine Department, The Royal Marsden Hospital, London, UK

[5]Targeted Approaches to Cancer Pain, The Institute of Cancer Research, London, UK

[*]**Corresponding author:** Giles SL, CRUK Cancer Imaging Centre, MRI Unit, The Royal Marsden Hospital, Sutton, Surrey SM2 5PT, United Kingdom, Tel: ; Fax: 0044 208 661 0846; E-mail: sharon.giles@icr.ac.uk

Received date: December 4, 2019; **Accepted date:** February 10, 2020; **Published date:** February 17, 2020

Citation: Giles SL (2020) Magnetic Resonance Guided High Intensity Focused Ultrasound (MrgHIFU) for Treating Recurrent Gynaecological Tumours: Effect of Pre-Focal Tissue Characteristics on Target Heating. J Imaging Interv Radiol Vol 3 No.1:1. DOI: 10.21767/2471-8564.3.1.1

Abstract

Objectives: To investigate temperature changes at the focus with various pre-focal fat/muscle tissues in both an experimental set-up and in patients treated with Magnetic Resonance guided High Intensity Focused Ultrasound (MRgHIFU).

Materials and Methods: Focal and pre-focal heating (Philips/Profound 3T Achieva MR/ Sonalleve HIFU system) were measured in an experimental set-up at 4, 6 or 8 cm depths with varying clinically-encountered tissue distributions. Six patients with recurrent gynaecological malignancy treated within a larger trial (NCT02714621) had intra-procedural temperature and thermal dose volume recorded.

Results: In the experimental set-up, focal heating of a target behind fat caused pre-focal heating. Achievable focal thermal dose volumes depended on pre-focal fat thickness: 8 cm required 9 kJ, 6 cm required 4.6 kJ and 4 cm required 2.7 kJ to achieve a 1.6 ± 0.5 ml ablated V_{30EM} volume. In comparison, a muscle only mimic of 8 cm thickness required 5.7 kJ. Layered fat/muscle mimic distributions caused greater temperature rises in the immediate, compared to the superficial, pre-focal region. In 2 patients with only pre-focal fat (1.4 cm and 5.9 cm thick respectively), 66°C at the focus with a measurable thermal dose volume (V_{240EM}=4.5 ml) was achieved in the former and 55°C without a measurable V_{240EM} in the latter. In 4 cases with tumours at 6.9-8.7 cm depth (median 7.9 cm) and an asymmetrical fat/muscle distribution, ablative temperatures (58°C) were only achieved in the shallowest tumour.

Conclusions: Increasing pre-focal fat thickness increases the power required to reach an ablative thermal dose. In tumours >7 cm deep to fat, ablation is limited. Symmetric or asymmetric layering of fat and muscle increases pre-focal heating.

Keywords: High-intensity focused ultrasound ablation; Magnetic Resonance Imaging; Ablation techniques; Genital neoplasms, female

Introduction

Gynaecological malignancies frequently recur with localized pelvic disease and cause progressive symptoms of pain and bleeding (1). Local treatment options are limited by the extent of previous surgery and radiotherapy, and by the site and extent of recurrence (2). The potential accessibility of different sites of recurrent gynaecological tumours to Magnetic Resonance guided High Intensity Focused Ultrasound (MRgHIFU) has been shown in prior work (3,4). However, the feasibility of delivering an ablative dose of thermal energy to these tumours located beneath variably thick layers of subcutaneous fat, muscle and intra-pelvic fat was not been assessed.

Difficulty in treating lesions deep to fat and muscle layers has been highlighted previously in renal tumours where layers of subcutaneous fat, muscle and peri-nephric fat are present (5,6). Problems arise because the attenuation coefficient of fatty tissues is higher than that of non-fatty soft tissues, e.g. muscle (7). Increased absorption causes fat to heat more, and differences in acoustic impedance between fatty and non-fatty soft tissues may cause reflection and refraction of ultrasound energy at tissue interfaces, further influencing the degree and

location of heating at the target. Temperature rises of >20°C at a target *in vivo* are required to achieve measurable thermal dose volumes and coagulative necrosis on histology (8). The purpose of this study, therefore was to investigate the temperature changes at the focus as a result of variable pre-focal fat/muscle tissues both in an experimental set-up (designed to address situations where fat/water tissue distributions are symmetric and asymmetric), and in patients treated with Magnetic Resonance guided High Intensity Focused Ultrasound (MRgHIFU).

Materials and Methods

This study used a Sonalleve HIFU device (Profound Medical, Ontario, Canada), integrated with a 3T Achieva MR scanner (Philips, Best, The Netherlands).

Experimental study

Tissue-mimicking models: Pre-focal tissue distributions in 3 scenarios seen clinically **(Figures 1a, 1b and 1c)** were simulated experimentally **(Figure 1d)**. Tissue-mimicking materials were selected for having clinically representative acoustic properties equivalent to fat and muscle **(Table 1)**, but were each water-based to allow MR-based temperature measurements within them using a proton resonance frequency shift (PRFS) thermometry technique (9). The shell of an emptied Sonalleve quality assurance (QA) phantom was used to mount all materials, which were inserted after the phantom shell had been partially filled with de-gassed water to ensure coupling without trapping air bubbles between layers. Tissue mimics were arranged inside the phantom in parallel-sided layers **(Figures 1d and 1e)** with a height-adjustable plunger on top to hold materials in place and to minimize water-filled gaps between buoyant layers.

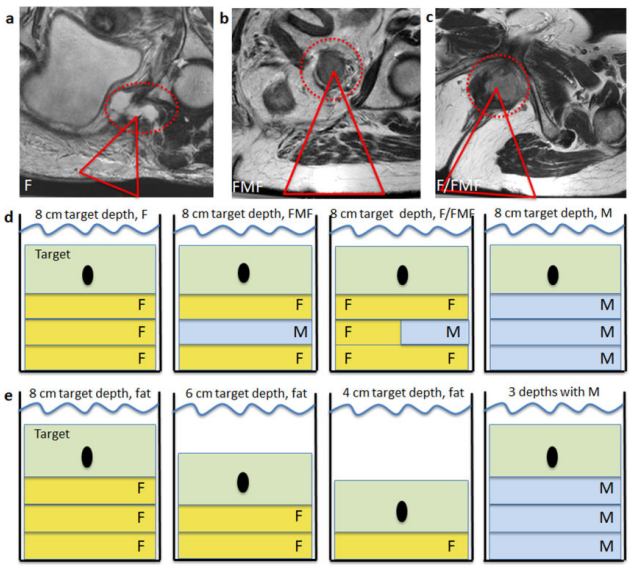

Figure 1: Axial T2W MRI showing pre-focal tissue distributions of fat and muscle in 3 clinical scenarios (a) homogeneous fat (F), (b) layered subcutaneous fat, muscle and intra-pelvic fat (FMF), and (c) an asymmetric distribution with fat alone on the medial side, and layered fat, muscle, and fat on the lateral side (F/FMF). Tumour targets are shown within the red dotted lines and the potential ultrasound beam path is represented simplistically by red triangles. In d and e, acoustic phantoms loaded with fat (F, yellow) and muscle (M, blue) tissue mimics are stylistically represented. These were used to assess depth dependent, and tissue distribution-dependent effects of pre-focal tissue composition on target ablation. The target (shown in green) includes the tumour (black ellipse). Each tissue mimicking layer was 2 cm thick to allow construction of 8 cm, 6 cm and 4 cm pre-focal layers. The model simulating a muscle only pre-focal environment is not encountered clinically, but was used to provide context to the results.

Table 1: Acoustic properties of human tissues at body temperature (* values as summarized by Duck (10-12)), and as measured for the tissue mimicking materials used in the experimental study. $Made in accordance with prior quality assurance (QA) work (14-22), by adding 5.5% by weight micron-sized (0.5-10 µm) silicon dioxide particles to a room-temperature solution of 2% agar in de-gassed, de-ionized water. The mixture was heated to 90°C under continuous stirring, maintained at that temperature for 10-20 minutes, before being cooled to approximately 45°C with stirring, and poured slowly into 2 cm thick, 15 cm diameter moulds, and allowed to solidify at 4°C. ^Cut from a QA phantom supplied by the National Physical Laboratory (23), ± cut from a Sonalleve QA phantom (24).

	Human tissue at body temperature*		Tissue mimicking materials		
	Fat	Non-fatty soft tissue	Fat mimic	Muscle mimic	Target material
Construction	-	-	Agar-silica gel$	Agar-based material^	Poly-acrylamide gel±
Propagation speed (ms^{-1})	1465	1575	1486 ± 0.7	1538 ± 1.2	1523 ± 3.3
Characteristic acoustic impedance ($\times 10^6$ $kgm^{-2}s^{-1}$)	1.44	1.66	1.56	1.72	1.60
Attenuation coefficient at 1 MHz ($dBcm^{-1}$)	1.0	0.6	1.16 ± 0.01	0.55 ± 0.01	0.38 ± 0.05
Attenuation coefficient frequency dependence	1.0	1.2	0.9	1.0	1.0

Assessment of depth dependent changes in focal and pre-focal heating: Treatment cells were placed wholly within the target material. These were 4, 6 and 8 cm from the base of the phantom for 2, 4 and 6 cm thicknesses of fat or muscle mimic **(Figure 1e)**. Following test exposures of 110 W for 16 s, 8 mm diameter 'regular' cells (20 s exposure duration) were delivered at an acoustic power that was increased in 20-30 W increments to 300 W (the maximum available). Additional higher energies were achieved by using 'feedback' cells to increase the duration of 300 W exposures to approximately 30 or 40 s. The 3 highest exposures were repeated 3 times with >10 min of cooling time between exposures.

Effect of pre-focal field distributions on focal and pre-focal heating: Targets lying 8 cm deep were exposed for each set-up. For the asymmetric model, cells were placed centrally, so that half of the beam passed through "fat", and half through "muscle". 8 mm diameter regular cells were exposed at 240 W and 270 W. This was followed by 3 sets of 300 W exposures delivered 3 times for each model. Exposure durations were 20 s for regular cells, and ~30 and ~40 s for feedback cells. At least 10 minutes cooling time was allowed between exposures.

Measurement methods

A PRFS sequence using an echo-planar imaging (EPI) accelerated, multi-slice 2D gradient echo T1-weighted technique was used to measure heating, using 7 mm thick slices: Four slices at the focus (3 coronal and 1 sagittal), and 1 coronal slice through the most superficial region of the lowest tissue-mimicking layer (to simulate the position of subcutaneous tissues) were used.

Experiments were conducted at room temperature (~21°C). The focal thermal dose volume (V_{30EM}) was estimated by measuring the product of the 3 orthogonal maximum dimensions of the 30 equivalent minutes at 43°C (EM) (10) dose contour. This cuboidal estimate was chosen for simplicity and to increase the range of measurable exposures compared to the elliptical dose volume provided automatically by the Sonalleve software, which is based on 240EM dose contours. Temperature change outside the focus was assessed by noting any 30EM or 240EM dose contours in the pre-focal region, and by recording the maximum temperature measured in the coronal superficial monitoring slice.

Clinical study

Patients: The patients included were the first 6 patients from a larger study (NCT02714621) investigating the use of the Sonalleve device. The study had approval from the institutional review board and was conducted in accordance with the principles of the Declaration of Helsinki, and Good Clinical Practice. Six patients aged (42-74 years, mean 61.1 years) with a proven diagnosis of symptomatic (pain, bleeding), recurrent gynaecological malignancy (2 endometrial, 2 vulvar, 1 cervix, 1 Bartholin's gland) provided their written, informed consent for treatment solely for the purposes of symptom palliation. Patients were not eligible for or had declined further surgery or radiotherapy. Tumour characteristics on the screening study were similar across all tumours: intermediate signal intensity, poorly enhancing tumours compared to neighbouring skeletal muscle in 5 cases and an enhancing nodule in 1 case. Imaging obtained at screening established baseline tumour volume, location and characteristics of pre-focal tissues. Reporting therapeutic pain response of the whole cohort from the study at its completion is outside the scope of this interim analysis which investigates heating at the focus in relation to pre-focal tissue composition.

Treatments: Patients were positioned with their target lesion as close as possible to the centre of the HIFU window; 4 patients with perineal, vaginal vault and pelvic sidewall lesions were in the supine-oblique position, whilst 2 patients with disease in groin regions were placed in a prone oblique position. Each had their exposed, depilated skin in direct contact with a chilled, dampened gel-pad that was in acoustic contact with the HIFU window. 3D-T1-W (TR 3.6 ms, TE=1.3, 2.4 ms, FA=10°, FOV 250 × 250 × 200 mm, SENSE=2 [RL] 1 [FH], NSA=3, 133 slices, scan duration 1 min 19 sec) and T2-W (TR 1500 ms, TE=165 ms, FA=90°, FOV 250 × 250 × 200 mm, SENSE=1.5 [RL] 2 [FH], NSA=1, 133 slices, scan duration 2 min 13 sec) were obtained before sonications and were used to plan treatments. In no patient was bone present in the far field to affect tumour heating.

After administration of sedation/anaesthesia (local/ regional nerve block in 1 case, conscious sedation in 2 cases and spinal anaesthesia with conscious sedation in 3 cases) and/or pain relief, treatments were delivered using regular and feedback cells of 4 mm and 8 mm diameter. PRFS data were obtained before, during and after each exposure to observe the temperature increases, and determine the required cooling time before the next exposure. Immediately after delivery of planned cells within the treatment volume, T2-W and T1-W images, before and after 0.2 ml/kg Gadolinium-based (Gd) contrast agent were re-acquired. Treatment duration ranged from 30.7-105.0 minutes (median 60.4 minutes). Further follow-up is part of the larger on-going trial.

Treatment assessment: The shortest distance from the skin to the centre of the planning target volume (PTV, which encompassed the tumour volume with the patient in the treatment position) represented the depth of the tumour targeted. The composition of pre-focal tissues **(Figure 1)** was classified as fat (F), layered fat/muscle/fat (FMF), or an asymmetric distribution (F/FMF). The total treatment volume (TV) was the cumulative volume of delivered cells. The power and duration of each sonication was used to calculate the total and the mean energy used during treatments.

PRFS data recorded maximum temperature at the focus. V_{240EM} was calculated as for V_{30EM} in the experimental study but was based on the more clinically relevant 240EM thermal dose contour because patients were at physiological temperature (~37°C). Pre-focal heating was assessed by noting the presence of any thermal dose contours outside the focal region.

Statistical analysis

Differences between temperature achieved and energy delivered in fat only vs. muscle only mimics were compared at

each depth using an independent samples t-test (GraphPad Prism software, version 7, San Diego, USA). Similar comparisons were made for pre-focal heating in the symmetric vs. asymmetric fat/muscle models.

Results

Experimental study

Pre-focal thickness and composition-dependent changes in target heating: The dependence of thermal dose volume (V_{30EM}) on pre-focal fat thickness is shown in **Figure 2a**. At 8 cm focal depth, with only fat pre-focally, V_{30EM} was 1.6 ± 0.5 ml for exposures using 300 W feedback cells for approximately 30 s (~ 9 kJ). In comparison, at 6 cm depth these thermal dose dimensions were achieved from exposures of ~4.6 kJ (230 ± 10 W), and at 4 cm depth from ~2.7 kJ (135 ± 15 W). The muscle only model required ~5.7 kJ (285 ± 15 W) for a target at 8 cm depth. Differences between fat and muscle models in energy required to achieve comparable thermal dose volumes were smaller at shallower target depths.

Pre-focal thickness and composition-dependent changes in pre-focal heating: There was increased measurable heating with decreasing focal depth/thickness of tissue mimics in the superficial monitoring slice that simulated the position of subcutaneous tissues **(Figure 2b)**. This occurred for both fat and muscle models, with higher pre-focal temperatures recorded in the former. Mean ± SD (range) temperatures for fat only model 40.6 ± 1.6 (38.3-43.7), 41.9 ± 1.5 (39.4-43.5), 48.4 ± 4.5 (42.7-53.3)°C at 8, 6 and 4 cm respectively, for muscle only model 38.7 ± 0.2 (38.5-39.1), 39.9 ± 0.9 (38.4-40.8), 42.2 ± 1.9 (39.5-44.4)°C at 8 cm, 6 cm and 4 cm respectively. However, differences between models were significant at 8 cm and 6 cm depth only p= 0.01, 0.04 and 0.06 at 8 cm, 6 cm and 4 cm.

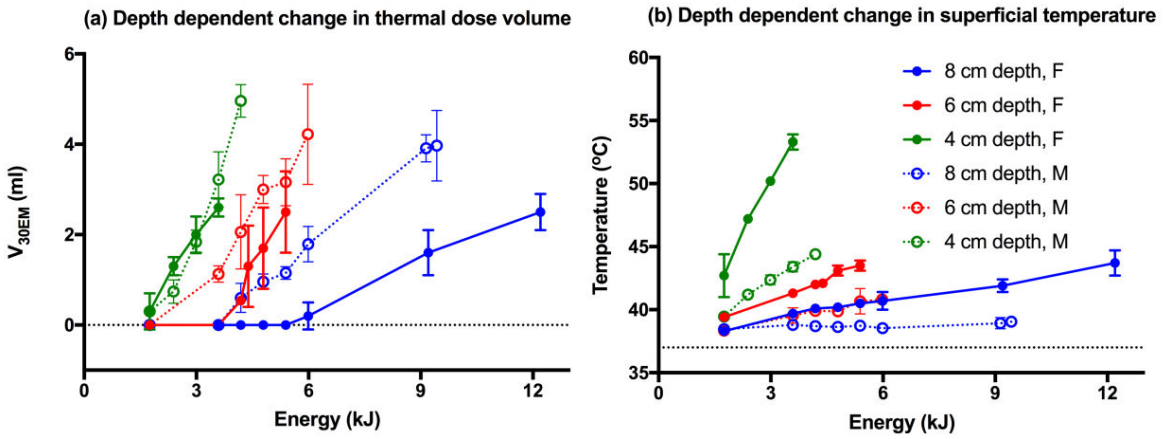

Figure 2: Depth dependent change for (a) thermal dose volume (V_{30EM}) and (b) superficial peak temperature in pre-focal fat (F) models (solid lines) versus muscle (M) models (dashed lines). Symbols and error bars show mean ± SD values for n ≥ 3 measurements. Energy was calculated as the product of acoustic power and total exposure duration; V_{30EM} was measured at the end of the cooling period after each exposure; superficial temperature was the highest value recorded in the monitoring slice at any time during or after the exposure.

When target heating was achieved, 30 and 240EM thermal dose contours were also seen pre-focally in the fat model for all focal target depths. At target depths of 8 cm, energies ≥ 6 kJ generated extensive thermal dose contours throughout the whole pre-focal region **(Figure 3a)**. At 6 and 4 cm depth, exposures of 4.6 kJ and 2.7 kJ respectively resulted in pre-focal heating only in the immediate pre-focal region **(Figure 3b)**, which was recognised as superficial at the shallower depth **(Figure 3c)**. In contrast, for the muscle model, 30EM dose contours were not seen outside the immediate pre-focal region, and no pre-focal 240EM dose contours were evident **(Figure 3d)**.

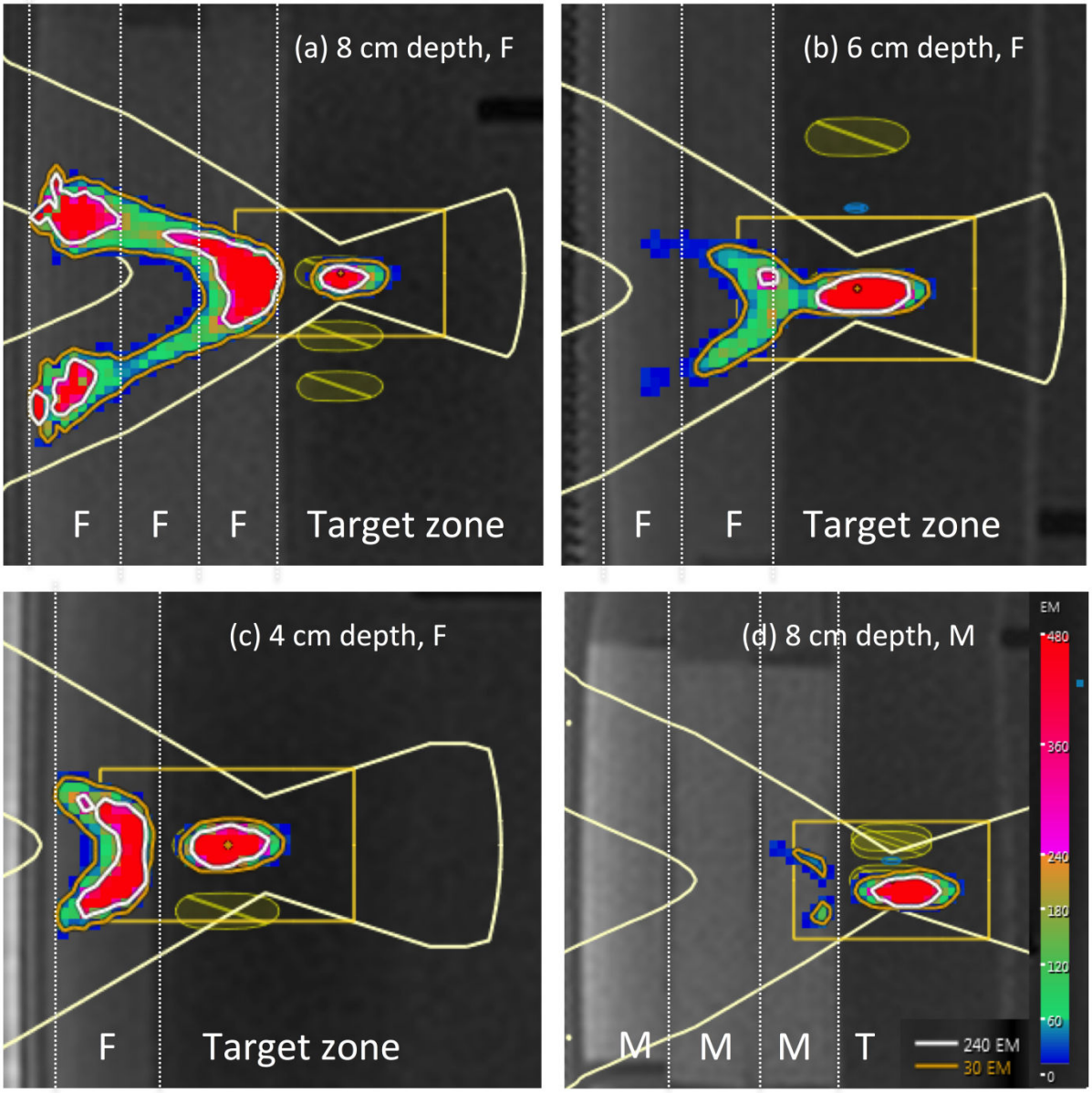

Figure 3: Thermal dose in focal and pre-focal regions at different depths. 30EM (orange contour) and 240EM (white contour) are shown for 300 W exposures made at depths of (a) 8 cm (b) 6 cm, and (c) 4 cm in the fat model, and (d) at 8 cm depth in the muscle model. The dashed white lines indicate the approximate positions of the interfaces between the fat (F) and muscle (M) mimicking materials (white letters) and the target zone (T). The apparent reduction of temperature in the middle fat mimicking layer at 8 cm depth results from a lack of thermometry slice at that location.

Effect of pre-focal tissue-mimic distributions on target and pre-focal heating: Superficial pre-focal temperatures (and resulting thermal dose volumes) were comparable for the fat only and layered models (F: 40.6 ± 1.6°C, FMF: 40.2 ± 1.4°C, F/FMF: 40.1 ± 1.6°C, **Figures 4a, 4b and 4c)**, but all were higher than in the muscle only model (38.7 ± 0.2°C). Compared to the fat-only model, the presence of the muscle-mimicking layer in the 3-layered symmetric model (FMF) qualitatively increased heating in the immediate pre-focal fat **(Figure 4b)** and decreased it in the superficial fat. In the asymmetric model (F/FMF), heating in the 'fat only' side of the model was equivalent in the superficial pre-focal regions, but it appeared intense and largely confined to the immediate pre-focal region on the '3-layered' side **(Figures 4c and 4d)**. Thermal dose volumes became measurable at exposures of ~6 kJ for each of the models (F, FMF, F/FMF) but were largest for the symmetric 3-layered model (FMF).

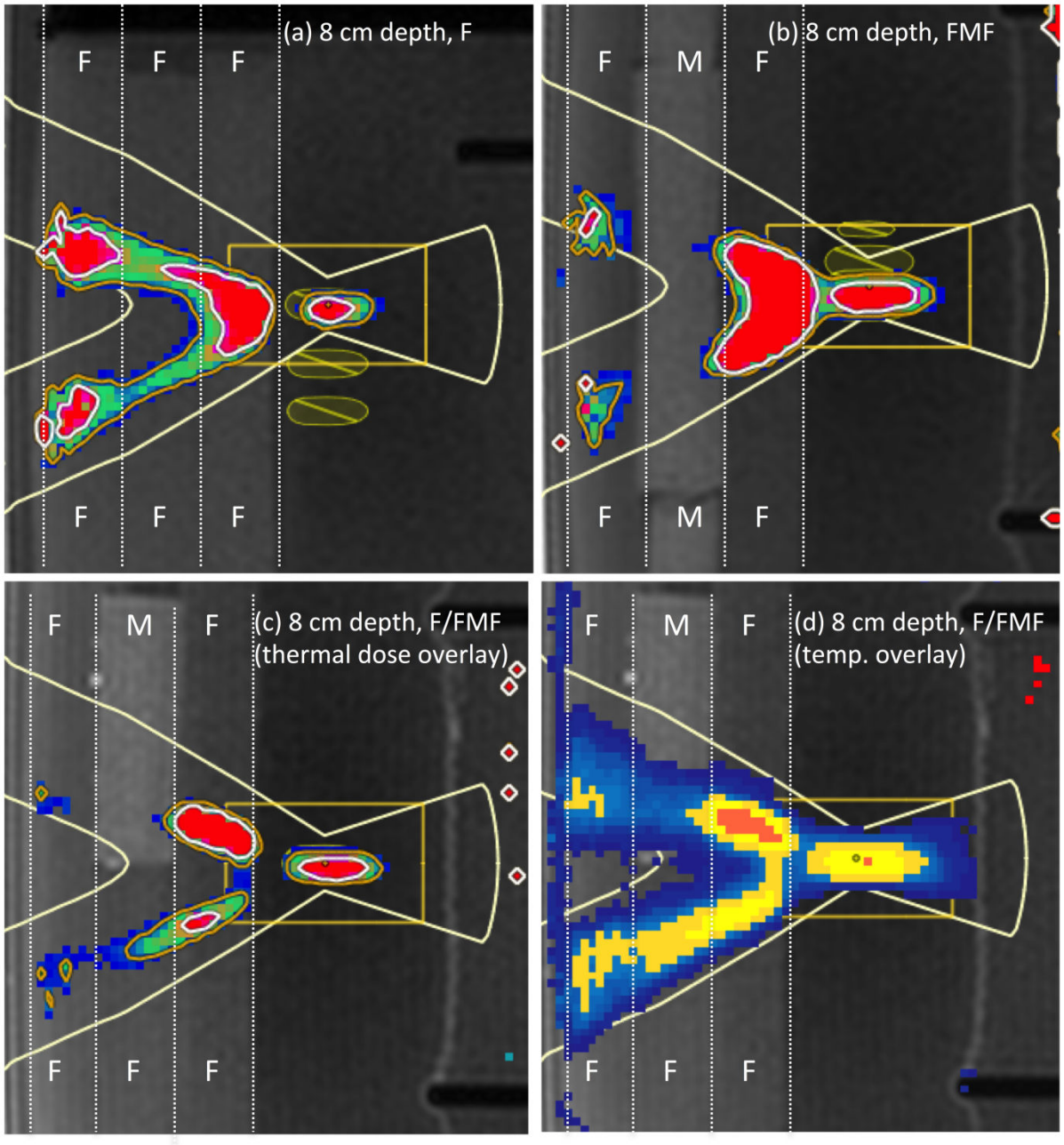

Figure 4: Thermal dose and temperature in focal and pre-focal regions for different pre-focal tissue distributions. 30EM (orange) and 240EM (white) thermal dose contours are shown for a 300 W, 40 s exposure made in (a) F, (b) FMF, and (c) F/FMF models. Image (d) shows the same exposure and model as image (c), but with the colour overlay in units of temperature (yellow and red pixels ≥ 56°C). The apparent reduction of temperature in the middle fat mimicking layer at 8 cm depth results from a lack of thermometry slice at that location. The asymmetry in images (c) and (d) suggests that the location of pre-focal heating is affected by the pre-focal fat/muscle distribution.

Clinical study

Baseline lesion characteristics and a summary of delivered treatment parameters for treatments in 6 patients are shown in **Table 2**.

Table 2: Treatment parameters and tumour characteristics for the clinical cohort. Note that tumour size was the maximum cross-sectional measurement and treatment energy was the cumulative value for the whole treatment. The planning target volume (PTV) did not necessarily encompass the whole gross tumour volume (GTV) if only a specific tumour region was targeted. Treatment volume (TV) was the cumulative volume of all delivered treatment cells and did not allow for any areas of overlap.

Patient ID:	18	22	23	24	25	22 #2	27
Tumour							
Size (mm)	11.9	35.6	62.7	50.8	35.2	46.6	55.5
Depth (mm)	69.3	86.9	54.5	81.7	14.7	79.1	76.4
GTV (ml)	1.2	23.6	59.4	13.4	24.0	41.1	28.6
Pre-focal tissues	F/FMF	FMF	F	F/FMF	F	FMF	FMF
Sonications							
Exposures/cells (n)	10/6	13/10	19/15	15/11	16/14	15/9	15/10
n × diameter (mm)	2 × 4, 4 × 8	8 × 4, 2 × 8	3 × 4, 12 × 8	2 × 4, 9 × 8	5 × 4, 9 × 8	3 × 4, 6 × 8	5 × 4, 5 × 8
Mean power (W)	198	179	225	216	77	209	200
Range power (W)	80-250	70-250	110-300	110-270	20-90	110-300	110-270
Treatment							
Energy (kJ)	36.35	38.88	80.34	61.68	23.32	95.58	52.84
PTV (ml)	3.2	43.9	23.3	47.1	30.5	65.8	17.8
TV (ml)	3.5	4.4	9.4	8.8	8.8	5.5	5.7
TV (as % GTV)	>100	18.5	15.8	65.8	36.7	13.2	19.9
TV (as % PTV)	>100	9.9	40.3	18.7	28.9	8.3	32.0
V_{240EM} (ml)	0.1	-	-	0.1	4.5	-	-
TM (°C)	58.3	51.2	54.5	50.0	66.3	46.6	47.8
Time (min)	30.7	57.2	64.9	55.9	70.6	120.7	105.0

Target ablation in relation to pre-focal tissue thickness and distribution: In 1 patient with 1.4 cm of pre-focal fat, a temperature of 66°C at the focus resulted in a measurable thermal dose volume (V_{240EM}=4.5 ml). The other patient with solely pre-focal fat (5.9 cm thick) achieved a temperature of 55°C but no measurable V_{240EM}. In 4 cases, where depth of tumours ranged from 6.9-8.7 cm (median 7.9 cm) with an asymmetrical fat/muscle distribution, ablative temperatures (58°C) were only achieved in the shallowest tumour. Therefore, focal temperatures ≥ 56°C, and measurable 30 and 240EM thermal dose volumes at the focus that are required for successful ablation without thermal dose contours outside the focus were seen in only 2 of 6 cases **(Figure 5)**. This was despite the use of 300 W, 40 s duration feedback cells. Heating of 43-47°C in the superficial tissues in these patients was insufficient to produce thermal dose contours **(Table 3)**. In one patient, treatment was prematurely curtailed because of PRFS thermometry indicating temperatures of 50°C at the skin. Immediately after treatment, changes in tumour GTV were seen in the 2 patients in whom there was a temperature increase of >56°C, likely related to oedema. No such increase in GTV was seen in the other 4 patients.

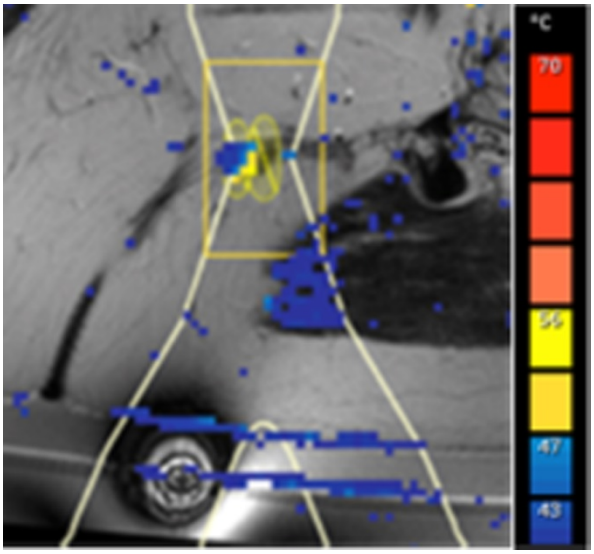

Figure 5: Pre-focal tissue distribution and MR thermometry in a patient with an asymmetric distribution of fat and muscle. Although the proton resonance frequency shift method could not indicate a temperature in the pre-focal fat, ablative temperatures and 240EM thermal dose contours were seen at the focus after a sonication of 250 W. In addition, blue pixels indicative of temperatures of 43-47°C were seen in the muscle on one side of the beam, and at both gel-pad interfaces (implying skin heating to this temperature also).

Table 3: Predicted energy loss in pre-focal muscle and fat mimics. Total attenuation is calculated as the product of attenuation coefficient and thickness of mimic. Attenuation power loss values are calculated by inserting the measured acoustic properties of the tissue mimicking materials into the intensity loss equation:, where I is the attenuated intensity (W/cm^2), I0 is the free field (unattenuated) intensity (W/cm^2), μ is the attenuation coefficient (dB/cm) of the tissue through which the ultrasound beam passes, and × (cm) is the distance over which the beam travels. Attenuation at a particular frequency is calculated as the product of attenuation coefficient and frequency (in this case 1.2 MHz) raised to the power of frequency dependence (0.9 and 1.0 for fat and muscle mimics, respectively). Power remaining is shown as the difference from 100%, and as the magnitude of power remaining from a maximal 300 W exposure.

Predicted energy loss through:	Total Attenuation (dB)	Attenuation power loss (%)	Power remaining (%)	Power (W) remaining from 300 W
2 cm muscle mimic	1.32	26	74	221
4 cm muscle mimic	2.64	46	54	163
6 cm muscle mimic	3.96	60	40	121
2 cm fat mimic	2.73	47	53	160
4 cm fat mimic	5.47	72	28	85
6 cm fat mimic	8.20	85	15	45

Discussion

We have demonstrated the limitations of delivering ablative doses to targets with varying distributions of pre-focal fat and muscle tissues in an experimental model, and in a pilot clinical study treating patients with recurrent gynaecological tumours in the pelvis. In the experimental set-up, focal thermal dose volumes were difficult to achieve at 8 cm depth with 6 cm pre-focal fat, even with 300 W, ≥ 6 kJ exposures. Consideration of the attenuation coefficients of the tissue mimics used relative to expected intensity reduction (10), would predict that less than 100 W would remain from 300 W after passing through ≥ 4 cm of fat mimic, whereas at least 120 W would remain even at 8 cm depth when muscle is the only pre-focal tissue. Displacement of the focus caused by the temperature-dependent speed of sound

demonstrated in porcine fat also should be considered when positioning the focus at the treatment site (5).

Pre-focal heating seen in the fat mimicking model, but not in the muscle-only model was probably related to increased absorption (11). This unwanted side-effect was problematic for both deep and shallow focal depths. Thus, pre-focal fat not only limits thermal ablation for deep-seated lesions, but also increases the risk of pre-focal tissue damage for shallow and deep lesions. In addition, layered distributions of fat/muscle/fat caused the immediate pre-focal region to heat considerably more than in fat and muscle only models. The more intense immediate pre-focal heating in these models is consistent with the lower attenuation of the muscle layer allowing more energy transfer, coupled with the relatively high absorption in the fat mimic.

Reports of other similar experimental work are sparse in the literature. The most relevant work has used excised porcine or human tissue. An immediate problem with the use of excised fat is that it changes consistency very rapidly outside the body, unless maintained under physiologically 'normal' conditions. Reported attenuation coefficients of porcine adipose tissue have ranged from 0.8 ± 0.1 dB/cm at 1 MHz (12) to 2.7 dB/cm at 1.1 MHz at 37°C (13), and of human perinephric fat from 0.8 dB/cm (14) to 1.35 dB/cm (5), The fat mimic used in these experiments, with an attenuation coefficient of 1.16 dB/cm at 1.2 MHz thus was within the correct range, but at the higher end of that reported for human fat (~0.5-1.5 dB/cm/MHz) (5,15-18) and therefore may have over-estimated energy loss related to attenuation. However, there was a smaller difference in sound speed and acoustic impedance between the fat and muscle mimics than in vivo **(Table 1)**, and so these experiments probably underestimated the estimated energy loss due to reflection and refraction. As in vivo human tissues are more heterogenous than the layers of tissue mimic, there is an anticipated increased potential for reflection and refraction leading to greater energy losses *in vivo*.

The energy losses demonstrated in the experimental study were borne out in the clinical study; treating through thicker layers of fat resulted in greater energy requirements in patients with deeper seated tumours compared to more superficial ones. However, the location of pre-focal temperature increases in a patient with a deep-seated (8 cm) tumour and a 3-layered (FMF) distribution treated with 300 W for 40 s was different to that seen in the tissue mimicking experiments. It occurred in the muscle and subcutaneous fat, but not in the immediate pre-focal region. Fascial layers also potentially alter the shape of the interface and may contribute to reflection of the ultrasound into the subcutaneous fat (19) In comparison, a patient in whom focal heating was achieved in a 1.2 ml tumour located 6-7 cm deep, had a tumour surrounded mainly by fat. Exposures in this patient (250 W for 20 s, 5 kJ) were within the range used to achieve measurable thermal dose volumes in the fat only model at 6 cm depth and indicated a lack of refraction in pre-focal tissues. Post-treatment skin erythema, and a region of presumed fat necrosis in the immediate pre-focal region in this patient was consistent with the uniform pre-focal heating seen in the experimental fat model.

There were several limitations to this study. There was uncertainty in absolute temperature measurement on MR thermometry from volume and temporal averaging. Also, although MR thermometry was not possible in fat in our clinical patients, in the experimental set-up we used a water-based fat mimic material to circumvent this and enable temperature measurement. However, the acoustic properties of the chosen materials may not have adequately mimicked the temperature dependence of tissues in vivo. Finally, experiments were designed to study simplified anatomical geometry where layers are uniform thickness and are parallel to each other and were performed at room temperature. Nevertheless, they indicate the crucially important pre-focal tissue composition and distribution factors that influence effective ablation in a clinical setting.

In the clinical cohort, the use of 'maximal' exposures available with the configuration of our Sonalleve system (300 W for 40 s using an 8 mm diameter cell) did not achieve ablative focal temperatures in the deepest tumours. Higher acoustic power settings (>700 W) are possible but not currently enabled for clinical HIFU treatments. It would be useful to establish whether using powers in excess of 300 W for a short duration offers any advantage for improving focal heating, without causing concurrent pre-focal damage. In addition, it may be possible to use other, differently configured extra-corporeal HIFU devices to improve dose delivery. The transducer focal length could be increased, and an actively coupled cooling system employed to achieve more effective target heating without the risk of skin burn. These devices are now available. Intra-cavitary HIFU devices for tumours in the vicinity of the vagina, bladder or rectum (20), would also be an advantage, circumventing the problem of subcutaneous and gluteal fat.

Conclusion

In conclusion, the thickness and distribution of fat and muscle in pre-focal pelvic tissues profoundly affects delivery of ablative doses to a tumour target. A >6 cm fat layer or asymmetric distribution of fat and muscle increases the risk of pre-focal heating and tissue damage in the beam path. In future, patient-specific pre-treatment modelling might allow better prediction of the thermal changes in deep-seated soft tissue lesions (21), so that methods of thermal dose delivery can be optimized.

Acknowledgements

We acknowledge NHS funding from the NIHR Research for Patient Benefit program (PB-PG-0815-20001), and to the NIHR Biomedical Research Centre and Clinical Research Facility in Imaging at the RMH, and the Cancer Research Network. Also CRUK and EPSRC support to the Cancer Imaging Centre at ICR and RMH in association with MRC & Department of Health C1060/A10334, C1060/A16464, equipment support from Philips Healthcare and Profound Medical, and ultrasound physics support from the Focused Ultrasound Foundation. The views expressed in this publication are those of the authors and not necessarily those of the NHS, the National Institute for Health Research or the Department of Health ans Social Care.

References

1. Kim YJ, Munsell MF, Park JC (2015) Retrospective review of symptoms and palliative care interventions in women with advanced cervical cancer. Gynecol Oncol 139: 553-558.
2. Ang C, Bryant A, Barton DP (2014) Exenterative surgery for recurrent gynaecological malignancies. Cochrane Database Syst Rev 2014: CD010449.
3. Machtinger R, Inbar Y, Ben-Baruch G (2008) MRgFUS for pain relief as palliative treatment in recurrent cervical carcinoma: a case report. Gynecol Oncol 108: 241-243.
4. Giles SL, Imseeh G, Rivens I (2019) MR guided high intensity focused ultrasound (MRgHIFU) for treating recurrent gynaecological tumours: a pilot feasibility study. Br J Radiol 92: 20181037.
5. Ritchie R, Collin J, Coussios C, Leslie T (2013) Attenuation and de-focusing during high-intensity focused ultrasound therapy through peri-nephric fat. Ultrasound Med Biol 39: 1785-1793.
6. Ritchie RW, Leslie T, Phillips R (2010) Extracorporeal high intensity focused ultrasound for renal tumours: a 3-year follow-up. BJU Int 106: 1004-1009.
7. Duck FA (2012) The propogation of ultrasound through tissue. In: ter Haar G, ed. The Safe Use of Ultrasound in Medical Diagnosis. 3rd edn. London: Br J Radiol 2012: 4-17.
8. Quesson B, Laurent C, Maclair G, de Senneville BD, Mougenot C, et al. (2011) Real-time volumetric MRI thermometry of focused ultrasound ablation in vivo: a feasibility study in pig liver and kidney. NMR Biomed 24: 145-153.
9. Rieke V, Butts Pauly K (2008) MR thermometry. J Magn Reson Imaging 27: 376-390.
10. ter Haar G, Coussios C (2007) High intensity focused ultrasound: Physical principles and devices. International Journal of Hyperthermia 23: 89-104.
11. Mougenot C, Kohler MO, Enholm J (2011) Quantification of near-field heating during volumetric MR-HIFU ablation. Med Phys 38: 272-282.
12. Goss SA, Johnston RL, Dunn F (1978) Comprehensive compilation of empirical ultrasonic properties of mammalian tissues. J Acoust Soc Am 64: 423-457.
13. Kyriakou Z, Corral-Baques MI, Amat A, Coussios CC(2011) HIFU-induced cavitation and heating in ex vivo porcine subcutaneous fat. Ultrasound Med Biol 37: 568-579.
14. Chivers RC, Hill CR (1975) Ultrasonic attenuation in human tissue. Ultrasound Med Biol 2: 25-29.
15. Cannon LM, Fagan AJ, Browne JE (2011) Novel tissue mimicking materials for high frequency breast ultrasound phantoms. Ultrasound Med Biol 37: 122-135.
16. Nasief HG, Rosado-Mendez IM, Zagzebski JA, Hall TJ (2015) Acoustic Properties of Breast Fat. J Ultrasound Med 34: 2007-2016.
17. El-Brawany MA, Nassiri DK, Terhaar G (2009) Measurement of thermal and ultrasonic properties of some biological tissues. J Med Eng Technol 33: 249-256.
18. Taniguchi DK, Martin RW, Myers J, Silverstein FE (1994) Measurement of the ultrasonic attenuation of fat at high frequency. Acad Radiol 1: 114-120.
19. Grisey A, Heidmann M, Letort V, Lafitte P, Yon S (2016) Influence of Skin and Subcutaneous Tissue on High-Intensity Focused Ultrasound Beam: Experimental Quantification and Numerical Modeling. Ultrasound Med Biol 42: 2457-2465.
20. Abel M, Ahmed H, Leen E (2015) Ultrasound-guided trans-rectal high-intensity focused ultrasound (HIFU) for advanced cervical cancer ablation is feasible: a case report. J Ther Ultrasound 3:21.
21. Suomi V, Jaros J, Treeby B, Cleveland RO (2018) Full Modeling of High-Intensity Focused Ultrasound and Thermal Heating in the Kidney Using Realistic Patient Models. IEEE Trans Biomed Eng 65: 2660-2670.
22. Partanen A, Mougenot C, Vaara T (2008) Feasibility of Agar-Silica Phantoms in Quality Assurance of MRgHIFU. ISTU; 2008, Minneapolis, MN, USA: AIP Conference Procedings.
23. National Physical Laboratory. Surface Temperature Test Phantom http://www.npl.co.uk/instruments/products/acoustics/surface-temperature-test-phantom/: National Physical Laboratory; 2018.
24. Computerized Imaging Reference Systems Inc. Ultrasound QA FAQS: http://www.cirsinc.com/support/ultrasound-qa-faqs; 2018.